Monomolecular Langmuir–Blodgett Films at Electrodes. Electrochemistry at Single Molecule "Gate Sites" †

Renata Bilewicz,‡ Takahiro Sawaguchi,§ Richard V. Chamberlain II, and Marcin Majda*

Department of Chemistry, University of California in Berkeley, Berkeley, California 94720

Received December 19, 1995. In Final Form: March 7, 1995⊗

The Langmuir–Blodgett (L-B) technique is used to coat electrode surfaces with bifunctional monolayer films that are designed to carry out two functions: passivation and gating. We demonstrate that incorporation of ubiquinone (Q_{50}) in otherwise passivating L-B monolayer films allows us to control access to the electrode surface via a controlled number of single molecule gate sites. The electrode passivation is accomplished with mixed octadecanethiol/octadecanol ($C_{18}SH/C_{18}OH$) monolayers, as described previously (Bilewicz, R.; Majda, M. *Langmuir* **1991**, *7*, 2794). A detailed characterization of the passivating properties of these L-B monolayers is provided in view of the Amatore-Saveant-Tessier (A-S-T) theory (Amatore, C.; Savéant, J.-M.; Tessier, D. *J. Electroanal. Chem.* **1983**, *147*, 39). The incorporation of low levels (10^{-12}–10^{-17} mol/cm^2) of ubiquinone allows electroreduction of probe species such as $Ru(NH_3)_6^{3+}$. At Q_{50} concentrations below 10^{-15} mol/cm^2, these monolayers behave as a random array of individual, 5-Å-radius disk microelectrodes each created by a single ubiquinone molecule. We postulate that a loose conformation of the ubiquinone's isoprenoid chain creates a channel that allows for a direct approach of $Ru(NH_3)_6^{3+}$ ions to the electrode surface. Electrochemical results are evaluated on the basis of A-S-T theory using direct comparison of the experimental and calculated cyclic voltammetric responses. Negative deviations in the observed voltammetric response compared with the theory at the Q_{50} concentrations higher than 10^{-15} mol/cm^2 are explained by postulating aggregation and loss of Q_{50} during L-B transfer.

Introduction

This report concerns the development of a Langmuir–Blodgett monolayer technique designed to control access to the electrode surface on a single molecule basis.

Selective response of the electrode/solution interface has been one of the major goals in electrochemistry.[1] Lack of selectivity in electrode reactions is, understandably, related to the lack of molecular character of the electrode/solution interface. Hence much research has been done to control the chemical nature of the interface by immobilization of chemical species at the electrode surface in order to manipulate its response. A number of reviews exist in the literature on this general subject.[2–6] Electroorganic synthesis is one of the areas of electrochemistry where control of the molecular character of the electrode/solution interface would result in significant benefits.[4,5] Of particular importance in electrosynthetic reactions is chiral selectivity. Strategies relying on the use of chiral solvents, supporting electrolytes, or adsorbates to create a chiral environment at the interface in order to predetermine the chirality of reaction products have been investigated.[4] Deliberate attachment of chiral reagents to the electrode surface has also been explored. The first example of such electrode modification was demonstrated by Miller et al., who covalently bound (*S*)-(−)-phenylalanine methyl ester.[7] Small chiral excess of a product was obtained in the electroreduction of 4-acetylpyridine using this "chiral electrode". In more recent studies, chiral effects in clay-modified electrodes and electrodes[8,9] coated with a chiral polymer, poly(L-valine),[10] have been reported in the literature. A degree of regioselectivity in electrosynthesis has also been reported in schemes involving cyclodextrin attachment at the electrode surface.[11] In most of these studies a lack of precise control of the chemical structure of the electrode/solution interface was responsible for the lack of full understanding of all the factors involved in the reaction mechanisms and the observed chiral effects.

More recently, the use of self-assembly and Langmuir–Blodgett methods in electrode modification have brought about better control over the structure of the electrode/solution interface. Several new schemes to induce selective response of the modified electrodes have been described. For example, some elements of charge selectivity were demonstrated by Crooks and co-workers, who self-assembled charged thiol compounds on gold electrodes.[12] pH dependent charge-selective response was observed by Nakashima in the electroreduction of ferricyanide at a gold electrode modified by self-assembly of

† Dedicated to Professor Dr. Hab. Zenon Kublik on the occasion of his retirement from Warsaw University.

‡ Permanent address: Department of Chemistry, Warsaw University, Pasteura 1, 02-093 Warsaw, Poland.

§ Current Address: JRDC Electrochemiscopy Project, Research Institute of Electric & Magnetic Alloys 2-2-1 Yagiyama-minami, Taihaku, Sendai 982, Japan.

⊗ Abstract published in *Advance ACS Abstracts,* May 15, 1995.

(1) Harrison, D. J.; Mallouk, T. E. in *Interfacial Design and Chemical Sensing*; Mallouk, T. E., Harrison, D. J., Eds.; ACS Symposium Series 561; American Chemical Society: Washington DC, 1994; Chapter 1, p 1.

(2) Bard, A. J. *Integrated Chemical Systems. A Chemical Approach to Nanotechnology*; J. Wiley and Sons, Inc.: New York, 1994.

(3) Bard, A. J.; Abruña, H. D.; Chidsey, C. R.; Faulkner, L. R.; Feldberg, S. W.; Itaya, K.; Majda, M.; Melroy, O.; Murray, R. W.; Porter, M. D.; Soriaga, M. P.; White, H. S. *J. Phys. Chem.* **1993**, *97*, 7147.

(4) Merz, A. In *Topics in Current Chemistry*; Springer Verlag: Berlin, 1990; Vol. 152, p 49.

(5) Fujihira, M. in *Topics in Organic Electrochemistry*; Fry, A. J., Britton, W. E., Eds.; Plenum Publishing Corp.: New York, 1986; Chapter 6, p 255.

(6) Murray, R. W. in *Electroanalytical Chemistry*; Bard, A. J., Ed.; M. Dekker Inc.: New York, 1984; Vol. 13, p 191.

(7) Watkins, B. F.; Behling, J. R.; Kariv, E.; Miller, L. L. *J. Am. Chem. Soc.* **1975**, *97*, 3549.

(8) Yamagishi, A.; Aramata, A. *J. Chem. Soc. Chem. Commun.* **1984**, *7*, 452.

(9) Bard, A. J.; Mallouk, T. In *Electroanalytical Chemistry*; Bard, A. J., Ed.; Marcel Dekker: New York, 1984; Vol. 13, Chapter 6, p 271.

(10) Komari, T.; Nonaka, T. *J. Am. Chem. Soc.* **1984**, *106*, 2656.

(11) Matsue, T.; Fujihara, M.; Osa, T. *J. Electrochem. Soc.* **1981**, *128*, 1473.

(12) Sun, L.; Johnson, B.; Wade, T.; Crooks, T. M. *J. Phys. Chem.* **1990**, *94*, 8869.

0743-7463/95/2411-2256$09.00/0

a dithiol derivative of diundecylphosphoric acid.[13,14] Umezawa and co-workers achieved ion-selective response by incorporating anion- or cation-binding species such as lipophilic macrocyclic polyamines or valinomycin in multilayer assemblies of phospholipid molecules.[15,16] Binding of "guest" anions or cations, respectively, induced some changes in the permeability of the electrode films by charged electroactive probe species such as $Fe(CN)_6^{3-}$ and $Ru(bpy)_3^{2+}$.

A more sophisticated ion-selective monolayer assembly was designed and reported by Rubinstein and co-workers.[17,18] Their monolayer system consisted of two components: 2,2'-thiobis(ethylacetoacetate) (TBEA) and *n*-octadecyl mercaptan co-self-assembled on a gold electrode. In this system electroactivity is limited to the TBEA sites since the octadecyl mercaptan forms an impermeable film. Under these conditions, ion-specific coordination of Cu^{2+} by TBEA, a necessary step in gaining access to the electrode surface, led to a selective electroreduction of cupric ions in the presence of ferric ions. A similar self-assembly scheme was also used recently by Kunitake and co-workers to immobilize a quinone derivative in an alkylthiol monolayer in order to carry out catalytic oxidation of NADH.[19]

This brief review of monolayer modification schemes suggests that future successes in this area will depend on the ability to control both the structure and composition of the surface monolayer assemblies. Immobilization of a range of different molecules, each purposefully chosen for a particular task and incorporated at a precisely controlled surface concentration, will be required to induce selective response of a modified electrode. To this end, we advocate the use of Langmuir–Blodgett (L-B) technique[20] as the method of monolayer deposition on the electrode surface. Unlike self-assembly, the L-B technique offers substantial flexibility in the choice of the species to be immobilize. This technique is not restricted, for example, to thiol derivatives, as is the case in self-assembly on gold and silver surfaces. Another important advantage of L-B transfer techniques is the ability to control precisely the composition of two (multi) component monolayers.

In a preliminary report, we have demonstrated the possibility of controlling access to an electrode surface through a controlled number of sites defined by single molecules referred to as "gate molecules".[21] Our approach involves deposition of a monomolecular L-B film designed to carry out two functions: passivation and gating.[22] A schematic structure of a L-B film deposited onto the electrode surface is shown in Scheme 1. The L-B monolayer consists of two types of molecules: long alkyl chain species, which are responsible for electrode passivation, and the gate molecules. Passivation is accomplished by monolayers consisting of 70 mol % of octadecanethiol (C_{18}-SH) and 30 mol % octadecyl alcohol as described previously

Scheme 1

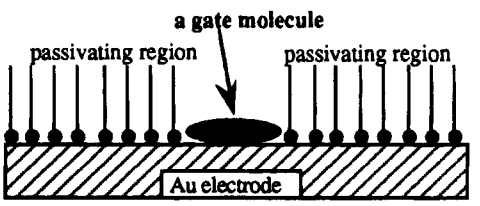

(see also the Experimental Section).[22] These two compounds combine their properties to form stable monolayers both at the air/water interface (due to high polarity of the hydroxyl groups) and on the gold electrode surface (due to octadecanethiol chemisorption). The passivating molecules form an ordered monolayer assembly which limits access to the electrode surface to a distance at which electron tunneling is negligibly slow. The single molecule marked as a gate in Scheme 1 represents those species which allow a closer approach to the electrode surface and thus define the sites of electroactivity. Their surface concentration can be controlled precisely by controlling the ratio of the long alkyl chain molecules and the gate molecules in the spreading solution used in the formation of the Langmuir monolayer at the air/water interface prior to its transfer onto the electrode surface. Since in this scheme of electrode modification the access to the electrode surface is limited only to the sites defined by the gate molecules, their structure could, in principle, be used to induce elements of *selective gating* on the basis of molecular size, charge, shape, and chirality.

In this report, we take advantage of the ability to control the surface density of the gate molecules in L-B films to correlate it with the magnitude of the electrochemical response in order to demonstrate our ability to control access to the electrode surface at the single molecule level.[21,22] Specifically, we describe the properties of ubiquinone (Q_{50}) as a gate molecule. Its structure is shown below.

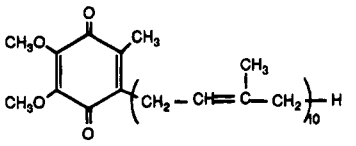

Q_{50}

In light of the fact that the area occupied by Q_{50} in surface monolayers (84 Å^2/molecule) is substantially larger than would be expected for this molecule with its chain in the most extended conformation, we postulate that the isoprenoid chain of ubiquinone adopts a conformation that functions as a molecular channel opening access to the electrode surface. We provide a quantitative analysis of the current voltage curves for the electroreduction of $Ru(NH_3)_6^{3+}$, a probe species, at the electrodes coated with bifunctional L-B monolayers of the type shown in Scheme 1. Surface concentration of the gate molecules is varied from 10^{-11} to 10^{-17} mol/cm^2. Finally, we compare our data with the predictions of the Amatore, Savéant, Tessier theory[23] and discuss discrepancies by postulating a mechanism that accounts for the loss of the gate molecules from the surface film at higher concentrations.

Experimental Section

Materials. 1-octadecanol (Aldrich, 99%) and 1-octadecanethiol (Aldrich, 98%) were triply recrystallized from 100% ethanol.

(13) Nakashima, N.; Taguchi, T.; Takada, Y.; Fujio, K.; Kunitake, M.; Manabe, O. *J. Chem. Soc. Chem. Commun.* **1991**, 232.
(14) Nakashima, N.; Taguchi, T. In *Interfacial Design and Chemical Sensing*, Mallouk, T. E., Harrison, D. J., Eds.; ACS Symposium Series 561; American Chemical Society: Washington DC, 1994; Chapter 13, p 145.
(15) Odashima, K.; Kotato, M.; Sugawara, M.; Umezawa, Y. *Anal. Chem.* **1993**, *65*, 927.
(16) Nagase, S.; Masamitsu, K.; Naganawa, R.; Komatsu, R.; Odashima, K.; Umezawa, Y. *Anal. Chem.* **1990**, *62*, 1252.
(17) Rubinstein, I.; Steinberg, S.; Tor, Y.; Shanzer, A.; Sagiv, J. *Nature* **1988**, *332*, 426.
(18) Steinberg, S.; Rubinstein, I. *Langmuir* **1992**, *8*, 1183.
(19) Kunitake, M.; Akiyoshi, K.; Kawatana, K.; Nakashima, N.; Manabe, O. *J. Electroanal. Chem.* **1990**, *293*, 277.
(20) Roberts, G., Ed. *Langmuir Blodget Films*; Plenum Press: New York, 1990.
(21) Bilewicz, R.; Majda, M. *J. Am. Chem. Soc.* **1991**, *113*, 5464.
(22) Bilewicz, R.; Majda, M. *Langmuir* **1991**, *7*, 2794.
(23) Amatore, C.; Savéant, J.-M.; Tessier, D. *J. Electroanal. Chem.* **1983**, *147*, 39.

Ubiquinone (Q_{50}) (Aldrich) was used without further purification. All other reagents were also used as received from the manufacturer: hexaaminеruthenium(III) chloride (Aldrich), chloroform (Fisher, ACS certified), perchloric acid (70% reagent grade, Aldrich), trifluoroacetic acid (Aldrich), and potassium chloride (Fisher, ACS grade). House-distilled water was passed through a four-cartridge Barnstead Nanopure II purification train consisting of Macropure pretreatment, Organics Free pretreatment, two ion-exchangers, and a 0.2 μm hollow fiber final filter for removing particles. The final resistivity of water used in the experiments was in the range 18.1–18.3 MΩ cm.

Hydrogenated Ubiquinone (HQ_{50}). Ubiquinone ($C_{59}H_{90}O_4$, 0.112 g, 0.130 mmol) was dissolved in 3 mL of ethyl acetate and stirred under ambient conditions for 180 min under a H_2 atmosphere in a standard hydrogenation apparatus in the presence of Pd/C (0.027 g, 10% Pd on activated carbon) catalyst. The resulting yellow solution was suction filtered through Celite on a sintered glass frit, and ethyl acetate was removed by evaporation *in vacuo*, leaving 0.101 g (88% yield) of an orange/yellow oil (HQ_{50}): ^{1}H NMR (C_6D_6, 500 MHz) δ 3.61 (s, 6, OCH_3), 3.38 (d, J = 4.4, 2, impurity), 2.37 (s, 1, impurity), 2.33 (t of d, J = 6.3, 2, methylene H α to ring), 1.79 (s, 3, methyl on ring), 1.54–1.40 (br m, 10, chain tertiary carbon protons), 1.48–1.28 (br m, 36, chain methylene protons), 1.18 (br m, 18, chain methylene protons β to tertiary carbons), 1.05 (d, J = 5.48, chain tertiary carbon protons), 0.93 (d, 33, chain methyl protons); ^{13}C NMR (C_6D_6, 125 mHz) δ 184, 183.8 (quinone carboxylic carbons), 143.1 (ring alkenyl carbons), 60.56, 60.23 (OCH_3), large group from 11.6 to 39.7 (chain carbons (ca. 2% impurity is due to residual unhydrogenated ubiquinone); TLC on silica gel support in 10/1 $CHCl_3$/heptane; single spot, R_f = 0.61; EI mass spectrum m/z 884 (M^+); Anal. Calcd for $C_{59}H_{110}O_4$: C, 80.20; H, 12.55. Found: C, 80.44; H, 12.22.

Electrode Fabrication, Pretreatment, and L-B Deposition Procedures. Pretreatment of gold substrates before L-B deposition is the most crucial element in the entire procedure for the preparation of L-B-coated electrodes. Electrodes were produced by vapor deposition of 70–100 nm gold films (99.95% Lawrence Berkeley Laboratory) at a slow rate, ca. 2–5 Å/s, onto glass microscope slides (Corning Plain Micro Slides) using a 1–5 nm thick chromium underlayer. We used a Veeco 7700 bell jar evacuated with a diffusion pump (using Santovac 5 UHV pump oil from Monsanto), operating at a base pressure of 1×10^{-7} Torr. Prior to the vacuum deposition of the metals, glass slides were washed in soapy water, rinsed thoroughly in Nanopure water, and then rinsed and boiled in 50:50 2-propanol/chloroform and dried. Electrode substrates were typically used in the L-B experiments within 7 week of their fabrication. They were stored in an evacuated desiccator in the intervening period.

Immediately before L-B coating, gold substrates were visually examined to select those electrodes free of any scratches or blemishes on the surface used later as the working area. The working electrode surface area was typically 0.36 cm^2. The cleaning procedure involved rinsing with organic solvents (chloroform, 2-propanol, acetone) and Nanopure water. Subsequently, gold substrates were immersed into a fresh, hot (ca. 80 °C) chromic acid solution for 30–60 s as a final cleaning step and in order to improve their wetability. Electrodes treated this way showed an open circuit potential in 1 M H_2SO_4 of +1.01 V vs a saturated calomel electrode (SCE), indicating that their surface is partially covered by surface oxide. L-B transfer of the $C_{18}SH/C_{18}OH$ monolayers on oxide-free gold substrates yielded somewhat inferior results due to reactive nature of the transfer process.[24] Significantly longer exposure to chromic acid increased the level of surface oxidation as judged by a positive shift of the open circuit potential. Those electrodes showed markedly poorer performance in the L-B deposition step. We believe that an excessive quantity of gold oxide is detrimental to the passivation function of our L-B films, as it prevents sulfur–gold bond formation. A more detailed assessment of the role of gold oxide in $C_{18}SH$ binding to gold during L-B deposition will be presented in a separate report.[25] The chromic acid treatment step was followed by a thorough rinse with nanopure water. Upon completion of this step, a wet gold substrate was immersed, within seconds (to minimize its contamination), into the water in a Langmuir trough.

Langmuir–Blodgett procedures and transfer protocol were described earlier.[24,26] $C_{18}SH/C_{18}OH$ monolayers (70:30 mol %) were spread initially at a surface concentration corresponding to 34–40 Å^2/molecule. Following solvent evaporation, the monolayer was compressed at a rate of 3.7 Å^2 molecule^{-1} min^{-1} to a pressure of 20–22 mN/m. The LB transfer was carried out at that pressure at a rate of 10 mm/min. Following the L-B transfer, the substrates were left in the nitrogen atmosphere of a Langmuir–Blodgett enclosure for several minutes before they could be transferred into an electrochemical cell or an enclosed glass container for later use.

Instrumentation. Langmuir and Langmuir–Blodgett experiments were carried out with a KSV Model 2200 system. The routine operating and maintenance procedures involved in these experiments were described before.[26] All electrochemical measurements were taken with a BAS 100A electrochemical analyzer (Bioanalytical Systems Inc.). Electrode potentials are references with respect to SCE.

Results and Discussion

1. Electrode Passivation with $C_{18}SH/C_{18}OH$ L-B Monolayers. The idea of carrying out electrochemical reactions at a collection of single molecule gate sites, as presented in Scheme 1, would allow one to interpret faradaic current, a macroscopic quantity, in terms of the number of microscopic events of electron transfer processes taking place at nearly identical, molecularly well-defined active sites dispersed across the electrode surface. At least two conditions have to be met to realize this idea. On one hand, the long alkyl chain molecules must form a passivating film on the electrode surface. More specifically, a background faradaic current due to electroreduction (oxidation) of a solution probe through the adventitious defect sites in the monolayer has to be smaller than that due to the smallest concentration of the gate molecules intentionally incorporated into an active monolayer assemblies. The other condition requires that the structure of a gate molecule and its orientation in the surface monolayer are such that a solution probe is allowed to approach the electrode surface sufficiently closely for the electron transfer to take place at an appreciable rate.

Since our original report,[22] the LB procedure presented in the Experimental Section has been used extensively in our studies of electrode passivation and in order to incorporate gate molecules. To illustrate the effectiveness of this procedure, we report here a summary of our passivation experiments carried out over a 6 month period and involving 70 electrodes. (This sample does not include a number of electrodes, ca. 10%, rejected at various stages of the fabrication and L-B deposition procedures before they were tested in the final electrochemical experiments.) We selected $Ru(NH_3)_6^{3+}$ as a probe species due to its large heterogeneous rate constant (see also section 5 below). Figure 1 shows three voltammograms recorded in 1 mM $Ru(NH_3)_6^{3+}$, 0.5 M KCl solution at the electrodes coated with passivating $C_{18}SH/C_{18}OH$ LB monolayers. These voltammograms are typical for 84% of the 70 electrodes mentioned above and represent a range of performance from the best to borderline passivation. (Ten electrodes that showed abnormally higher currents were rejected.) The approximate likelihood of obtaining such results is the following: curve a, 30%; curve b, 35%; curve c, 35%.

In order to treat these results more quantitatively, we used a mathematical model of Amatore, Savéant, and Tessier (A-S-T)[23] describing voltammetric current at an

(24) Krysinski, P.; Chamberlain, R. V., II; Majda, M. *Langmuir* **1994**, *10*, 4286.
(25) Chamberlain, R. V., II; Majda, M. Unpublished results.
(26) Lindholm-Sethson, B.; Orr, J. T.; Majda, M. *Langmuir* **1993**, *9*, 2161.

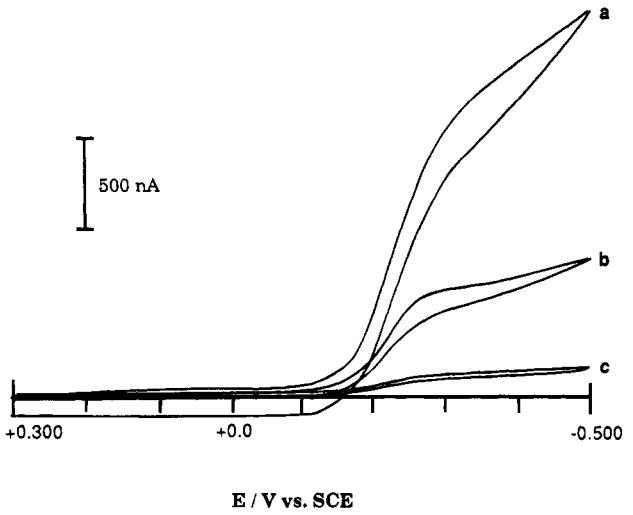

Figure 1. Test of electrode passivation. Cyclic voltammetry of 1.0 mM $Ru(NH_3)_6^{3+}$ recorded in 0.5 M KCl solution (v = 50 mV/s) on gold electrodes (A = 0.25 cm^2) coated with $C_{18}SH/C_{18}OH$ (70:30 mol %) LB monolayer films. These voltammograms represent typical results corresponding to (a) 30%, (b) 35%, and (c) 35% of individual electrodes in a large series of the L-B experiments (see the text).

array of microelectrodes (a detailed description of the model is given in section 2). For a case of a hexagonal array of microdisk electrodes spaced sufficiently far apart from each other so that their individual diffusion layers do not overlap, the theory gives the following equations describing the magnitude of the plateau current and the shift of the half-wave potential with respect to a reversible value:

$$E_{1/2}-E^{\circ\prime} = \frac{RT}{\alpha F}\ln[0.6R_0D^{-1}(1-\theta)^{1/2}k_{app}] \quad (1)$$

$$i_{lim} = FSC^*D(1-\theta)^{1/2}/0.6R_0 \quad (2)$$

$$1-\theta = (R_a/R_0)^2 \quad (3)$$

where R_a is the disk radius, $2R_0$ is the interdisk spacing, and θ is the passive fraction of the electrode surface. On the basis of this theory (eq 1), we calculated an apparent value of R_a of the defects in the passivating L-B film assuming k_{app} = 80 cm/s. The latter was obtained for $Ru(NH_3)_6^{3+}$ at an electrode coated with Q_{50} containing L-B films (see section 5). This is a reasonable approximation considering the fact that in both cases $Ru(NH_3)_6^{3+}$ approaches the electrode surface through a pinhole-like channel. As discussed in section 5 below, the value of k_{app} is dominated by double layer effects, which should be similar in both cases. Equation 2 was then used to calculate R_0 and the effective concentration of the defect sites. This data analysis allows us to describe the passivating properties of the $C_{18}SH/C_{18}OH$ L-B monolayers in terms of a particular surface concentration (Γ) and size (R_a) of defect sites modeled as disks. Specifically, the analysis of the voltammograms in Figure 1 yielded the following values of Γ and R_a: curve a, 6.7 × 10^{-17} mol/cm^2, 6.2 Å; curve b, 1.2 × 10^{-17} mol/cm^2, 8.1 Å; curve c, 2.6 × 10^{-18} mol/cm^2, 8.3 Å. For the sake of comparison, we also carried out the same experiments with 12 gold electrodes (treated identically to those in the L-B experiments) coated with self-assembled $C_{18}SH$ monolayers according to a literature procedure.[27] They gave comparable passivation results (Γ in the range from 0.8 to 2 × 10^{-17} mol/cm^2, $R_a \approx 7$ Å).

The picture of the structure of our L-B monolayers emerging from the application of the A-S-T theory in this analysis is somewhat simplified. For example, the radii of the defect sites appear to be excessively large. A disk with an 8 Å radius corresponds to an area occupied by about 10 closely packed $C_{18}SH$ molecules. Clearly, the determination of the radius of the defects (eq 1) is burdened with an error due to uncertainties in the measurements of $E_{1/2}-E^{\circ}$. Furthermore, since the surface concentration calculated from the magnitude of the plateau current (eq 2) is inversely proportional to R_a, the actual Γ may be as much as a factor of 2 higher. It is also important to note that the voltammograms in Figure 1 have slightly sloping plateaus due to kinetically controlled $Ru(NH_3)_6^{3+}$ reduction current. Thus, the LB monolayers contain, in addition, a number of smaller defect sites ("weak spots") which allow reduction of the ruthenium probe via electron tunneling.[28] With these uncertainties in mind, the A-S-T model gives us, nevertheless, a useful semi-quantitative means of assessing passivation characteristics of our LB monolayers which is particularly useful, for example, in relative comparisons of different batches of electrodes and in testing procedural modifications. In view of the low level of defects in the LB monolayers (defect density of 1 × 10^{-17} mol/cm^2 corresponds to one defect site per 17 μm^2), it is unlikely that their source is related to the grain boundaries in the vapor-deposited gold films. Preliminary AFM/STM studies of our gold films showed 30 nm in diameter smooth hill-and-valley type grains having peak to valley elevation differences of approximately 50 Å. We believe, therefore, that the pinhole defects are created by traces of impurities on the gold surface and/or by impurities present in the $C_{18}SH/C_{18}OH$ Langmuir monolayers prior to the L-B transfer.

Each series of L-B transfer experiments involving Q_{50} included at least two "blank" electrodes coated with $C_{18}SH/C_{18}OH$ passivating monolayers that contained no gate molecules. The level of passivation obtained in this way indicated the minimal level of the gate molecules that could be incorporated in the L-B films in that series so that faradaic background current would not exceed 20% of the $Ru(NH_3)_6^{3+}$ reduction current at the lowest level of gate molecules.

2. Electrochemistry at Single Molecule Gate Sites. Incorporation of ubiquinone molecules in the L-B monolayers opens access to the electrode surface through the otherwise passivating film and yields a voltammetric response consistent with that expected for an array of microelectrodes.[21] In this section, we deal with the electrochemical data documenting this type of behavior of the monolayer-coated electrodes. The mechanistic aspects of the functioning of the individual gate molecules are discussed in section 4.

A series of the cyclic voltammograms of 1 mM $Ru(NH_3)_6^{3+}$ in 0.5 M KCl solution obtained at the gold electrodes coated with $C_{18}SH/C_{18}OH/Q_{50}$ is shown in Figure 2 for Q_{50} surface concentration in the range from 8 × 10^{-18} to 10^{-13} mol/cm^2. One observes sigmoidal-shaped voltammograms at low Q_{50} surface coverage which adopt a progressively more peak-like shape as the Q_{50} surface concentration increases. This trend reflects a progressively higher extent of overlap between the hemispherical diffusion zones developed around individual gate sites as their surface concentration increases.[23]

(27) Becka, A. M.; Miller, C. J. *J. Phys. Chem.* **1992**, *96*, 2657.

(28) Miller, C. J.; Cuendet, P.; Gratzel, M. *J. Phys. Chem.* **1991**, *95*, 877.

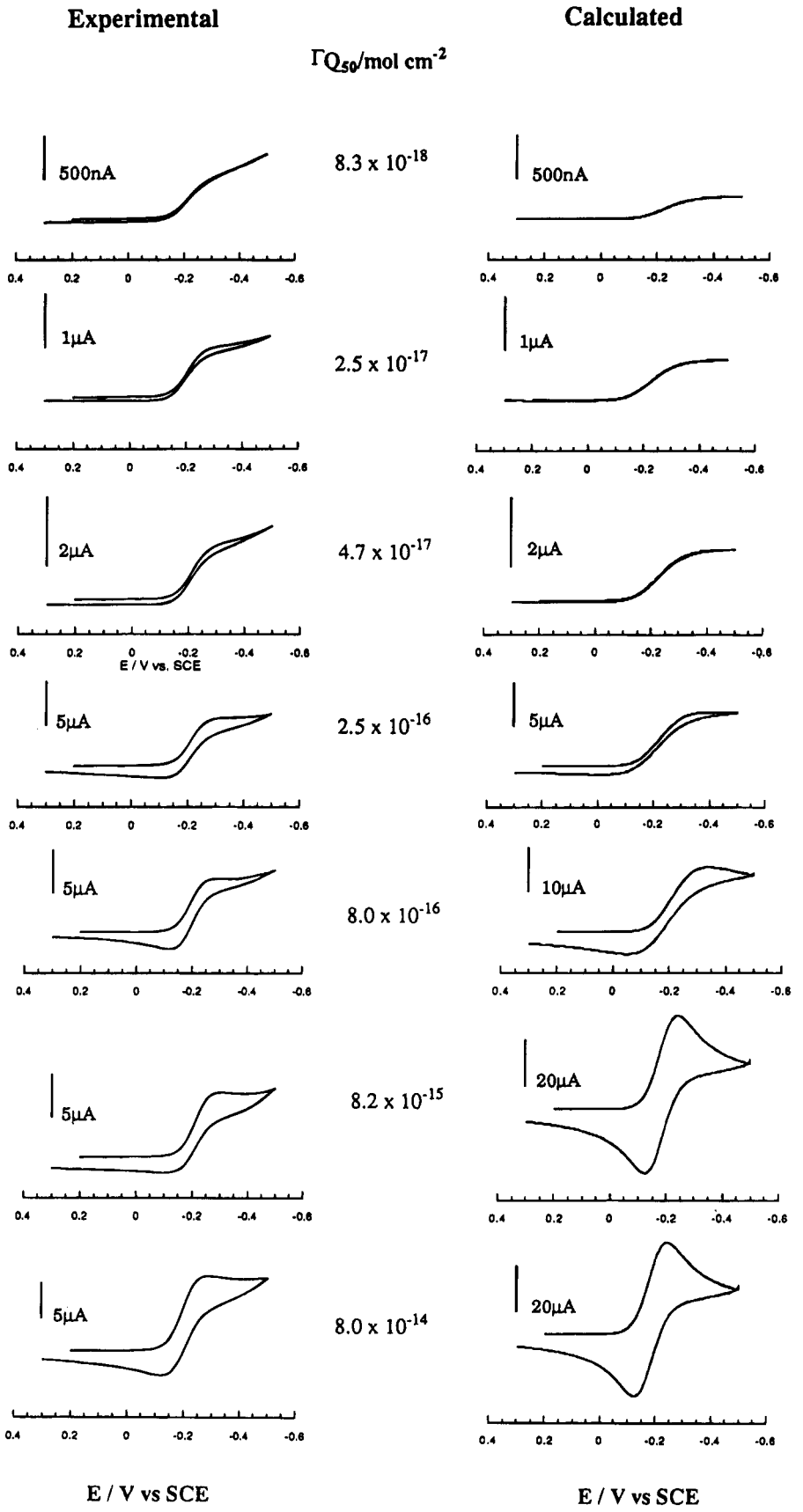

Figure 2. Comparison of the experimental and calculated cyclic voltammograms of 1 mM $Ru(NH_3)_6^{3+}$ recorded on gold electrodes coated with $C_{18}SH/C_{18}OH$ L-B monolayer films containing an increasing concentration of Q_{50}. The experiments were carried out in 0.5 M KCl solutions at 0.36 cm^2 electrodes at $v = 50$ mV/s. The calculations were done according to eqs 4–9 (see the text) using the same experimental parameters and $E^0 = 0.180$ V vs SCE, $D = 6.0 \times 10^{-6}$ cm^2/s, $k_{app} = 80$ cm/s, and $R_a = 5.0$ Å.

The quantitative evaluation of the voltammograms of the type shown in Figure 2 was done on the basis of A-S-T theory.[23] They derived a general equation for the voltammetric current at a hexagonally arranged array of microdisk electrodes (R_a in radius). The master integral equation for the dimensionless voltammetric current when

$\theta \rightarrow 1$ is given by eq 4:

$$\psi = \Lambda(1-\theta)\exp(\alpha\xi)\{[1 - I\psi - A\psi] - [I\psi + A\psi]\exp(-\xi)\} \quad (4)$$

in which

$$\psi = \frac{i}{FSC^*\left(\frac{DFv}{RT}\right)^{1/2}} \quad (5)$$

$$\Lambda = k_{app}\left(\frac{RT}{DFv}\right)^{1/2} \quad (6)$$

$$A = 0.6R_o\left(\frac{DRT}{Fv}\right)^{-1/2}(1\text{-}\theta)^{-1/2} \quad (7)$$

$$\xi = -\frac{F}{RT}(E - E^\circ) \quad (8)$$

$$I\psi = \pi^{-1/2}\int_0^\tau \frac{\psi}{(\tau - \eta)^{1/2}}\,d\eta \quad (9)$$

and, where θ is the passivated fraction of the electrode surface area, D, C^*, α, and k_{app} are the diffusion coefficient, bulk concentration, transfer coefficient, and the heterogeneous electron transfer rate constant of the redox probe species; v is the voltage scan rate, and the other symbols have their usual meaning.

Using the numerical algorithm of Matsuda and coworkers,[29] we used eq 4 to obtain numerically the theoretically expected current–voltage curves. A small sample of the calculated voltammograms is also shown in Figure 2. We used a literature value[30] of 6×10^{-6} cm^2/s for the diffusion coefficient of $Ru(NH_3)_6^{3+}$, $v = 50$ mV/s, and our experimentally obtained value of 80 cm/s for the apparent rate constant, k_{app}. This value of k_{app} is most likely affected by double layer effects as discussed in section 5. However, it was measured under the conditions described in Figure 2 and thus its use as an apparent value in these calculations is internally self-consistent and appropriate. The values of $(1 - \theta)$ and R_a were those that we obtained from the Langmuir experiments for mixed $C_{18}SH/C_{18}OH/Q_{50}$ monolayers. thus, we assumed that the concentration and the size of the gate molecules were the same as those obtained from pressure vs area isotherms on the water surface before a monolayer was transferred onto the electrode surface (see also discussion in section 4).

Comparison of the experimental and calculated cyclic voltammograms for the $C_{18}SH/C_{18}OH/Q_{50}$ system in Figure 2 shows good agreement between both sets of curves in terms of their shape as it changes from sigmoidal to that characteristic for a linear diffusion process with increasing Q_{50} concentration. However, a progressively increasing negative error in the current magnitude in the experimental set of curves becomes conspicuous as Q_{50} surface concentration approaches and exceeds 10^{-15} mol/cm^2. In order to compare quantitatively the experimental results of the type shown in Figure 2 with the numerical calculations, we measured the maximum voltammetric current (peak current or plateau current depending on the shape of the voltammograms) and plotted them vs the logarithm of Q_{50} surface concentration in Figure 3A. Figure 3B shows the same results replotted in terms of current per gate molecule, i/N, vs their surface concentration in the L-B monolayers. The latter format of plotting the experimental results clearly shows the effect of the radial diffusion component on the current magnitude at a single gate molecule. As the concentration of the gate sites decreases, one observes an increase in the diffusion controlled current per Q_{50} molecule as hemispherical diffusion begins to dominate mass transport. Of most interest is the plateau region at surface concentrations below 10^{-15} mol/cm^2. In this region, each gate molecule behaves independently of its neighbors; in other words, the average separation between them is large enough to assure no significant overlap between the individual hemispherical diffusion zones. Under these conditions, the total current is simply a sum of the current passed at each gate sites:[31]

$$i_{total} = \sum_N 4nFR_aDC^* \quad (10)$$

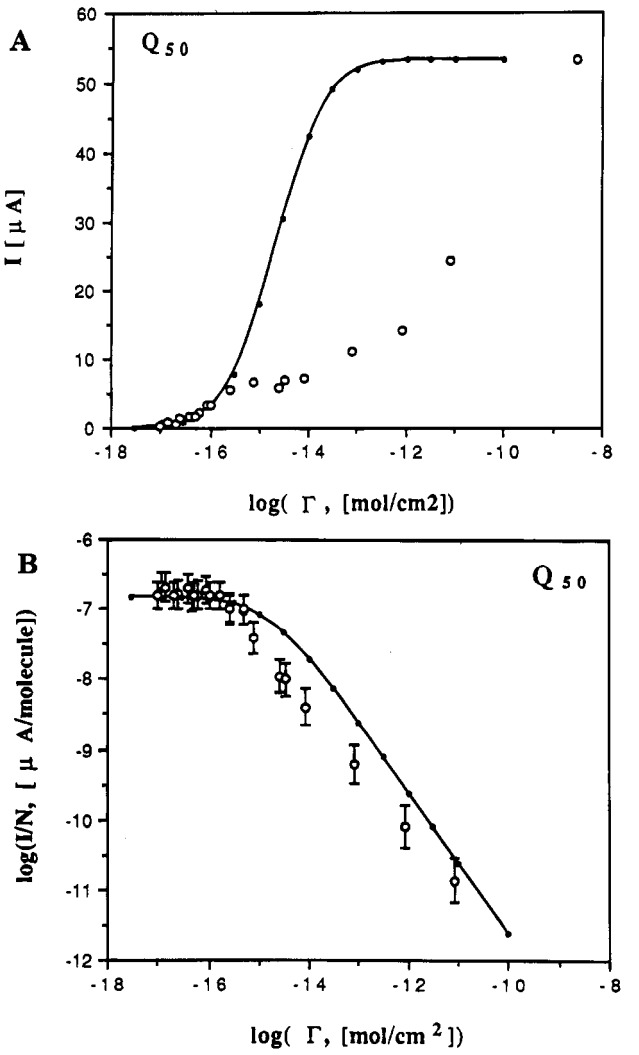

Figure 3. Comparison of the experimently measured (open circles) and the calculated (close circles and the connecting solid line) values of the peak (plateau) currents for a series of experiments illustrated in Figure 2. The experimental conditions and the parameters used in the calculations are the same as those listed in Figure 2. (A) absolute values of current vs logarithm of the surface concentration of Q_{50} in the L-B monolayers. The data point at log $\Gamma = -8.5$ represents the peak current value of a voltammogram recorded on a clean gold electrode. (B) the same set of data replotted as a logarithm of current per Q_{50} molecule in the L-B monolayers. The error bars represent standard deviations of 7–12 measurements on different electrodes.

(29) Guechi, T.; Tekenda, K.; Matsuda, H. *J. Electroanal. Chem.* **1979**, *101*, 29.
(30) Gennett, T.; Weaver, M. J. *Anal. Chem.* **1984**, *56*, 1444.

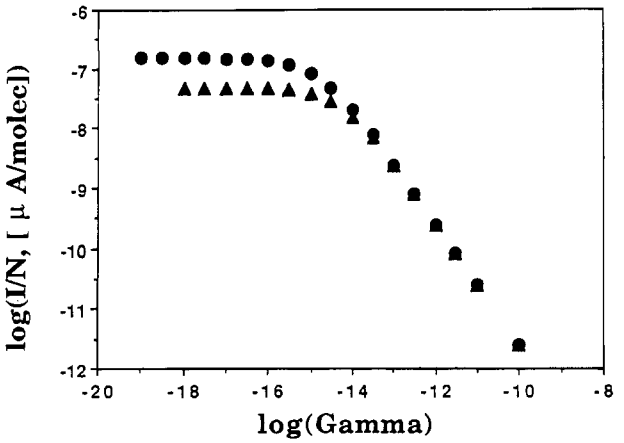

Figure 4. The effect of aggregation of the gate molecules. Comparison of the calculated values of the peak (plateau) current for the reduction of 1.0 mM $Ru(NH_3)_6^{3+}$ on electrodes coated with $C_{18}SH/C_{18}OH$ monolayer L-B films containing variable concentrations (Γ) of Q_{50}: Circles, conditions identical to those in Figure 3B, no aggregation; triangles, aggregation number $n = 10$.

Using R_a values of 5 Å obtained from Langmuir experiments at the air/water interface (see discussion below), eq 8 predicts $i/N = 1.2 \times 10^{-13}$ A while the average experimental value in the plateau region in Figure 3 is $2.0 \pm 1.4 \times 10^{-13}$. The rather poor precision of the average values of the current/gate molecule in the plateau region is due to the uncertainties in the background current as discussed above.

3. Deviations from the Predictions of A-S-T Theory. As pointed out above, a large negative deviation from the theory can be observed in the experimental data sets in Figure 3A,B, at the surface concentrations of Q_{50} exceeding ca. 10^{-15} mol/cm^2. We considered two types of phenomena in our attempt to account for this departure from the theory. One is aggregation of the gate molecules in the monolayer at the air/water interface that can take place immediately after spreading when all molecules have substantial lateral mobility due to their low surface concentration. This could result in the formation of a smaller number of larger aggregates of Q_{50}. The other postulate assumes a loss of ubiquinone.

To test the first postulate, we carried out some additional computations of the current–voltage curves according to eq 4 incorporating aggregation of the gate molecules characterized by the aggregation number, n (a number of molecules forming a single larger active site). Naturally, the number density of the active sites becomes n times smaller than the known surface density of the gate molecules used in an experiment. The radius of the aggregated active sites was approximated simply by $\sqrt{n}R_a$. The results of these calculations are shown in Figure 4 for $n = 10$ in terms of a $\log(i/N)$ vs $\log \Gamma$ plot (N is still the total number of gate molecules inserted in the L-B monolayer). As expected, in the plateau region, where the current level is not affected by the overlap of the diffusion zones around individual active sites, i/N is smaller by $\sqrt{10}$ compared to the case with no aggregation. However, these calculations show that there is no difference in the behavior of the system in the higher concentration region of the active sites. In that region, the decreased number of sites is compensated by a more effective (involving a larger hemispherical component) mass transport. It is clear therefore, that simple aggregation does not explain the deviations observed in Figure 3.

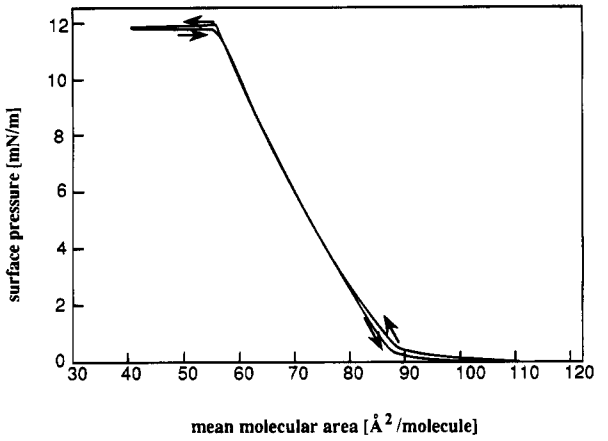

Figure 5. The compression/decompression isotherm of Q_{50} on pure aqueous subphase; $T = 21$ °C.

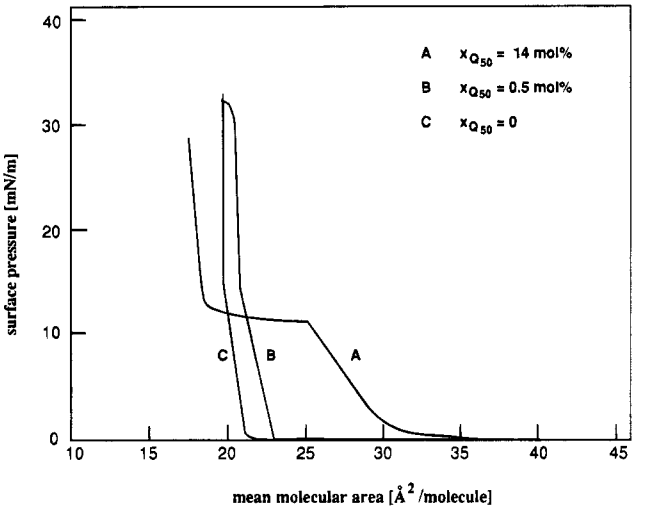

Figure 6. Pressure–area isotherms of mixed Q_{50}–$C_{18}SH/C_{18}$-OH monolayers on pure aqueous subphase; $T = 21$ °C; the mole fractions of Q_{50} are listed in the figure.

We must, therefore, consider a loss of Q_{50} from the monolayer or their deactivation as the mechanisms that would account for the decreased values of current observed at higher gate site concentrations. The excellent stability of Q_{50} Langmuir monolayers at low pressures on the water surface assures us of the insolubility of this compound in water, which otherwise could explain its loss. Therefore, we postulate that the loss takes place via aggregation which is then followed by either deactivation or a "squeezing out" mechanism during monolayer compression at the air/water interface and/or during the subsequent L-B transfer. Instability of pure Q_{50} monolayers at pressures above 11 mN/m can be clearly seen in Figure 5. The monolayer collapses at 12 mN/m. Regardless of the extent of collapse of Q_{50} monolayers, reversal of the barrier motion leads to respreading of Q_{50} along exactly the same isotherm as in the compression direction. This reversible character of collapse/respreading processes suggests that the collapsed state of this material is liquid. Figure 6 shows π–A isotherms of mixed $Q_{50}/C_{18}SH/C_{18}$-OH monolayers. The shape and the large difference in the area per molecule at 10 and 20 mN/m of an isotherm, A, corresponding to a large mole fraction of Q_{50} suggest that self-segregation of Q_{50} molecules into separate domains leads to their collapse and squeezing out at ca

(31) Wightman, R. M.; Wipf, D. O. In *Electroanalytical Chemistry*; Bard, A. J., Ed.; Marcel Dekker: New York, 1989; Vol. 15, p 267.

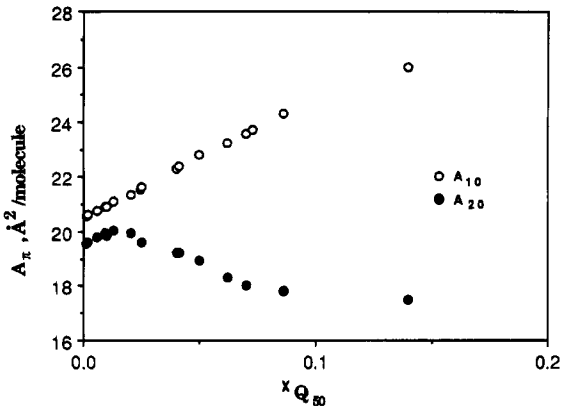

Figure 7. Plots of the average molecular areas at 10 and 20 mN/m (open and closed circles, respectively) vs mole fraction of Q_{50} obtained from π–A isotherms of mixed Q_{50}–$C_{18}SH/C_{18}OH$ monolayers on pure aqueous subphases.

12 mN/m. This is consistent with the behavior of a pure Q_{50} monolayer (Figure 5). This effect is less severe, however, as the mole fraction of Q_{50} is decreased below ca 2 mol % (isotherm B).

A quantitative analysis of this behavior is presented in Figure 7, where we plot the average area per molecule measured at 20 mN/m and at 10 mN/m as a function of Q_{50} mole fraction in the Langmuir monolayer. For an ideally behaved two-component system, the average area per molecule at both pressures could be expressed by the following equation:

$$A_\pi = x_{C_{18}SH/C_{18}OH}A_{C_{18}SH/C_{18}OH} + x_{Q_{50}}A_{Q_{50}} \qquad (11)$$

where x and A are the mole fractions and the areas per molecule of the two components, measured at a particular pressure, π. The slope of the line drawn through the data points collected at π = 10 mN/m gave the Q_{50} molecular area of 63 Å^2/molecule. This is in good agreement with the molecular area for Q_{50} obtained for that pressure from a pure Q_{50} isotherm which is 61 ± 2 Å^2/molecule. The negative slope of the plot obtained at 20 mN/m illustrates the squeezing out effect. However, the large negative deviation in this data set is observed only at $x_{Q_{50}} \gtrsim 0.02$, suggesting that as the mole fraction of Q_{50} decreases below 2 mol % its self-segregation leads to the formation of smaller aggregates which can no longer be squeezed out completely. However, Q_{50} aggregation, followed by partial squeezing out of the monolayer, may be possible even at surface concentrations as low as 10^{-15} mol/cm^2. Thus, we postulate that the negative deviation of the current magnitude compared with the theory in Figures 2 and 3 is due to aggregation and subsequent loss of Q_{50}. In addition, self-segregation may also lead to deactivation of the aggregates as viable gate sites via, for example, changes of orientation with respect to the plane of the monolayer.

4. Mechanism of Q_{50} Functioning as a Gate Molecule. Considering the structure of Q_{50} shown in the Introduction, it is difficult to predict the conformation that this molecule adopts in the L-B monolayer. A hint of a possible conformation is provided by the cross sectional area that Q_{50} occupies on the water surface of 84 ± 2 Å^2 (see Figure 5) independent of solution pH. This is substantially larger than a projected area an isoprenoid chain would occupy in an all-trans conformation oriented vertically with respect to the water surface. The latter can be estimated to be less than 40 Å^2/molecule. This suggests that the isoprenoid chain of Q_{50} may form an opening channel in the monolayer by adopting a substantially looser conformation. Since the radius of $Ru(NH_3)_6^{3+}$ is approximately 3.6 Å,[32] it seems plausible that the channel is large enough to allow direct access of the ruthenium probe to the electrode surface.

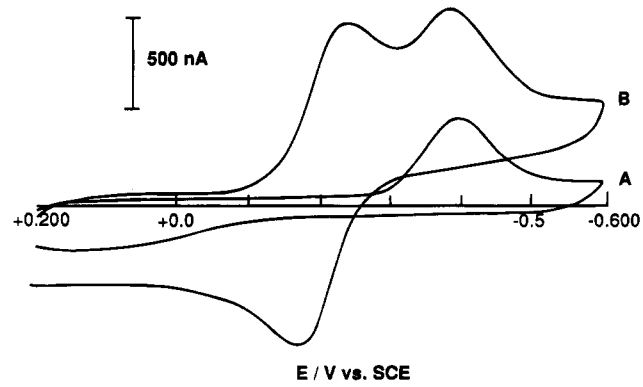

Figure 8. Cyclic voltammograms recorded in the absence (curve A) and in the presence (curve B) of 2 × 10^{-5} M $Ru(NH_3)_6^{3+}$ on a gold electrode (A = 0.36 cm^2) coated with a $C_{18}SH/C_{18}OH$ LB monolayer containing 2 mol % of Q_{50}; 0.5 M KCl, v = 50 mV/s.

We next consider the possibility of mediated electroreduction of $Ru(NH_3)_6^{3+}$ by ubihydroquinone, as it could be an important element in the functioning of Q_{50} as a gate molecule. The direct electroactivity of ubiquinone in L-B monolayers can be recorded if its surface concentration is 1 mol % or higher. In 0.1 M NaOH solutions, Q_{50} exhibits reversible 2e$^-$ surface waves[33,34] which served to establish excellent correlation between its concentration in the L-B monolayer at the electrode surface and at the water surface prior to the L-B transfer.[22] In solutions with pH < 10, the electrochemistry of ubiquinone involves 2e$^-$, 2H$^+$ and results in kinetically irreversible behavior characterized by a large separation of the cathodic and anodic peak potentials.[33,34] Figure 8 (curve A) presents a voltammogram of Q_{50} (at 2 mol % in a $C_{18}SH/C_{18}OH$ monolayer) recorded in a neutral pH, 0.5 M KCl solution. The same electrode was then used to record a voltammogram following addition of $Ru(MH_3)_6^{3+}$ at 2 × 10^{-5} M (Figure 8, curve B). Since the peak potential of the Q_{50} reduction is nearly 200 mV more negative than the redox potential of the $Ru(NH_3)_6^{3+/2+}$ couple, it is clear that ubiquinone is not engaged in the mediation of $Ru(NH_3)_6^{3+}$ reduction.

Electron tunneling between $Ru(NH_3)_6^{3+}$ and the electrode surface through Q_{50} is the next possibility to be considered. This would involve electronic states of the isoprenoid chain's five double bonds. Janzen and Bolton postulated that ubiquinone functions as "molecular wire" on the basis of their tunneling junction experiments involving multilayer L-B assemblies of chlorophyll, stearic acid, and ubiquinone.[35] To test this hypothesis, we catalytically hydrogenated all the isoprene units (see the Experimental Section) and then tested the electrochemical behavior of $Ru(NH_3)_6^{3+}$ at the monolayer-coated electrodes incorporating hydrogenated ubiquinone (HQ_{50}). Following catalytic hydrogenation, HQ_{50} can be compressed on the water surface to a substantially higher surface pressure (21 mN/m) than Q_{50}. Its collapse at that pressure has the same characteristics of a liquid film as those described above for Q_{50}. The limiting area obtained from the π–A isotherms is 67 Å^2, a smaller value than 84 Å^2 obtained

(32) Sutin, N.; Brunschwig, B. S.; Creutz, C.; Winkler, J. R. *Pure Appl. Chem.* **1988**, *60*, 1817.
(33) Petrova, S. A.; Kolodyazhny, M. V.; Ksenzhek, O. S. *J. Electroanal. Chem.* **1990**, *277*, 189.
(34) Schrebler, R. S.; Arratia, A.; Sanchez, S.; Haun, M.; Duran, N. *Bioelectrochem. Bioenerg.* **1990**, *23*, 81.
(35) Janzen, A. F.; Bolton, J. R. *J. Am. Chem. Soc.* **1979**, *101*, 6342.

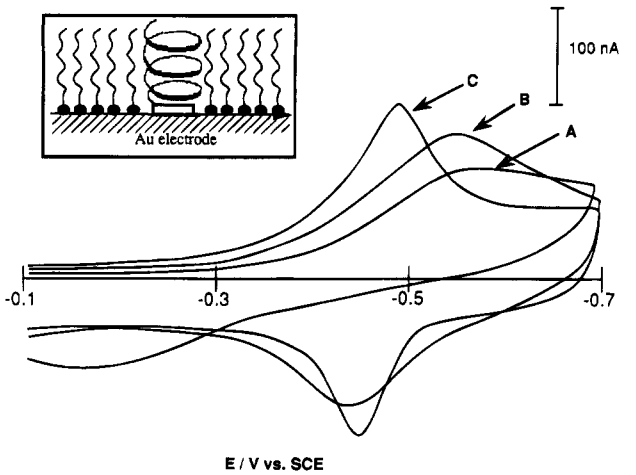

Figure 9. Cyclic voltammograms of Q_{50} immobilized (1.5 mol %) in a $C_{18}SH/C_{18}OH$ L-B monolayer on a gold electrode surface ($A = 0.36$ cm^2). A, 0.4 M TBAOH; B, 0.4 M TBAOH + 0.02 M K_2SO_4; C, 0.4 M TBAOH + 1.0 M K_2SO_4; $v = 50$ mV/s. The inset is a cartoon of a Q_{50} molecule showing how a loose conformation of its isoprenoid chain might create an opening channel in a passivating $C_{18}SH/C_{18}OH$ monolayer.

for Q_{50}. This is consistent with a more flexible character of the alkyl chain compared to its isoprenoid precursor.

The electrochemical behavior of HQ_{50} incorporated at the 7.6 mol % level in the $C_{18}SH/C_{18}OH$ monolayers at pH 11 was nearly superimposable with that due to Q_{50} under the same conditions. This assures us that the quinone moiety of Q_{50} withstood intact the hydrogenation procedure. The result of a crucial experiment in which the electrochemical behavior of $Ru(NH_3)_6^{3+}$ was examined at a $C_{18}SH/C_{18}OH$-coated electrode with the HQ_{50} gate sites at the surface concentrations below 10^{-15} mol/cm^2 produced, within the experimental error, the same results as those featured in Figure 2, for which Q_{50} was used as gate species. Thus we conclude that long range electron transfer is not involved in the reduction of $Ru(NH_3)_6^{3+}$ at the Q_{50} gate sites.

In view of these results, we believe that Q_{50} opens access to the electrode surface by creating a channel in the $C_{18}SH/C_{18}OH$ monolayer that is defined by a favorable, dynamic average conformation of the Q_{50} isoprenoid chain. The key element in this model is a postulate that $Ru(NH_3)_6^{3+}$ is reduced at a close proximity to the electrode surface and that neither the quinone group nor the isoprenoid chain play a detectable role in this process. Thus, in principle, we cannot rule out the possibility that $Ru(NH_3)_6^{3+}$ is reduced at defect sites in the L-B monolayer created by the Q_{50} molecules. The coiled structure of the isoprenoid chain shown in the inset to Figure 9 is merely intended to illustrate the idea of an open channel and does not stem from a structural characterization. Whether this channel is capable of imposing a size limitation on the species approaching the electrode surface, as the drawing in Figure 9 might suggest, remains an open question.

While these types of studies are in progress, we report here an element of "size selectivity" in the electrochemical behavior of Q_{50} itself. As shown before, electroreduction of Q_{50} immobilized in a $C_{18}SH/C_{18}OH$ monolayer in an alkaline electrolyte is a 2e− process.[22] Consequently, it requires two cations to be brought into the proximity of the quinone group to match the charge of the Q^{2-} group. In other words, the countercations participating in this process must enter the channel Q_{50} creates just as we postulated $Ru(NH_3)_6^{3+}$ does. Figure 9 shows cyclic voltammograms of 1.5% Q_{50} in a $C_{18}SH/C_{18}OH$ L-B monolayer

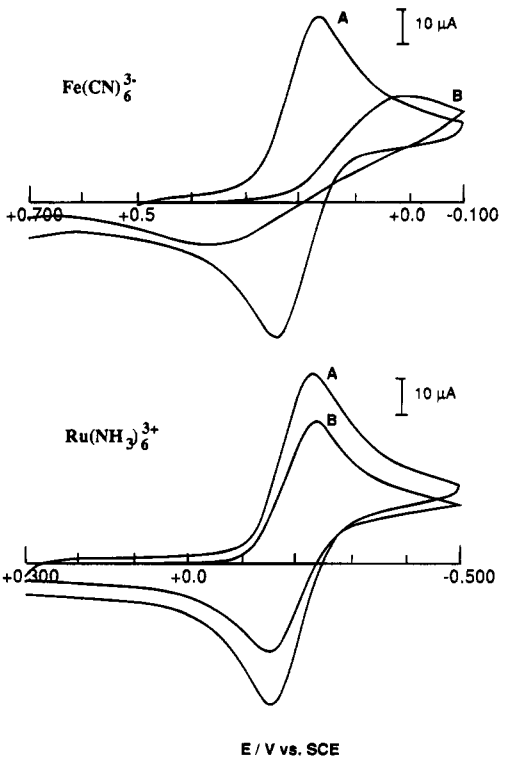

Figure 10. Comparison of the cyclic voltammetric behavior of $Fe(CN)_6^{3-}$ and $Ru(NH_3)_6^{3+}$ in 0.5 M KCl solutions on a bare gold electrode (curves A) and on a gold electrode coated with a $C_{18}SH/C_{18}OH$ LB monolayer containing 4.4×10^{-13} mol/cm^2 of Q_{50} (curves B); $A = 0.36$ cm^2, $v = 50$ mV/s.

recorded in tetrabutylammonium hydroxide (TBAOH) solutions. It is clear that the otherwise reversible 2e$^-$ reduction/oxidation of Q_{50} is severely impeded (Figure 9A) when TBA^+ is the only available countercation. Apparently TBA^+ ions are too bulky to access the quinone moiety through the isoprenoid channel. Addition of K_2SO_4 to the electrolyte alleviates the problem of size-dependent accessibility of countercation and returns the electrochemistry of Q_{50} to its normal (Figure 9C) reversible behavior. The requirement of a large excess of K^+ ions (compare curves B and C) suggests that due to their hydrophobicity TBA^+ ions partition into the surface layer and partially block access of potassium ions.

5. Kinetics of the Heterogeneous Electron Transfer at the Gate Sites. The small size of the gate molecules creates conditions of extremely high mass transport rates in the experiments where the surface concentration of the gate molecules is in the plateau region (Figures 2 and 3B; $\Gamma < 10^{-15}$ mol/cm^2). Under these conditions, one can approximate the mass transport coefficient, m_o, by D/r, where r is the radius of a gate site.[31] Considering the value of r yielding $m_o = 100$ cm/s, it becomes clear that the electrochemical behavior of almost all redox couples should be kinetically controlled. For example, in Figures 10 and 11 we compare the electrochemical behavior of ferricyanide and ruthenium hexamine ions at the same electrodes coated with L-B monolayers that contain 4.4×10^{-13} and 5.2×10^{-17} mol/cm^2 of Q_{50} gate molecules, respectively. In the former case (Figure 10), a relatively high Q_{50} concentration generates smaller mass transport rates than in the experiments featured in Figure 11. However, in both cases, these results show that the kinetic facility of the ferri/ferrocyanide couple is not sufficiently high to yield a well-developed voltammogram under these conditions. The literature reports place the apparent heterogeneous rate constants of $Fe(CN)_6^{3-/4-}$ in the range 0.01−0.1 cm/s, depending on the state of the electrode

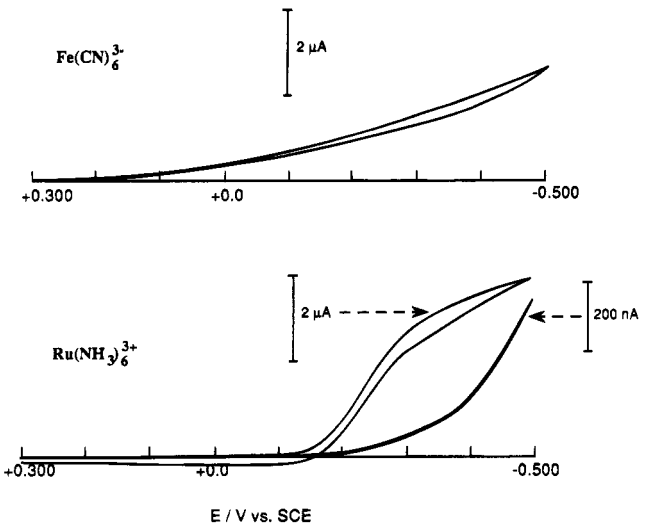

Figure 11. Comparison of the voltammetric behavior of $Fe(CN)_6^{3-}$ and $Ru(NH_3)_6^{3+}$ in 0.5 M KCl solutions on a gold electrode coated with a $C_{18}SH/C_{18}OH$ L-B monolayer containing 5.2×10^{-17} mol/cm^2 of Q_{50}. For comparison, the lower panel also contains a voltammogram recorded at a 10 times higher sensitivity in the same $Ru(NH_3)_6^{3+}$ solution at an electrode coated with a passivating $C_{18}SH/C_{18}OH$ L-B film not containing any Q_{50}.

and the type and concentration of the supporting electrolyte.[36-39] On the other hand, the apparent rate constant for the $Ru(NH_3)_6^{3+/2+}$ couple was reported to be from ca. 0.4 cm/s[30,40] to 1.2 cm/s.[41] (Rate constants of this magnitude border on the upper limit of the kinetic capabilities of the electrochemical methods.)

A-S-T theory provides a simple means of measuring an apparent rate constant of the electron transfer. Namely, in the plateau region of Figure 3B, eq 1 describes the magnitude of the shift in $E_{1/2}$ of a steady-state current voltage curve with respect to the formal potential, ΔE. The measured values of ΔE of -39 ± 1 mV for Q_{50}-containing systems yield an apparent rate constant of the electron transfer of 80 ± 2 cm/s. These values, together with those reported recently by Penner et al. at nanometer-sized microelectrodes (79 ± 44 cm/s),[42] are the highest reported for this redox couple in the literature. We believe that the unusually high values of our rate constant are likely due to double layer effects.[43]

A quantitative evaluation of these effects is very difficult if not impossible as it would require knowledge of the potential of zero charge, E_z, as well as the potential in the diffuse layer at the plane of electron transfer, E_{pet}. The former can be estimated on the basis of the literature data for clean gold electrodes.[44] At the gold [111] surface in KCl electrolytes, $E_z \cong +0.1$ V vs SCE.[44,45] However, the magnitude of the diffuse layer potential cannot be simply calculated as φ_2 on the basis of Gouy–Chapman–Stern theory[43] due to the complicated and not well-understood nature of the gate sites and their effect on the double layer structure. We can only postulate that the magnitude of E_{pet} can be expected to be higher than that at an uncoated electrode under the same electrolyte conditions since the hydrophobic nature of the isoprenoid chain and the channel it forms may restrict access of water and K^+ ions. In spite of these uncertainties, it is, nevertheless, useful to estimate the magnitude of the correction and the true rate constant, k_s^t, assuming a certain plausible value of E_{pet} and using the classical Frumkin correction equation:[43]

$$k_s^t = k_{app} \exp(z_o - \alpha n) F E_{pet}/RT \qquad (12)$$

It is apparent that if E_{pet} were to be -0.03 V, the true standard rate constant, k_s^t, would be ca. 4 cm/s (using $\alpha = 0.5$), a value similar to that reported in the literature.[30] The physical significance of the Frumkin correction involves a higher concentration of $Ru(NH_3)_6^{3+}$ at the PET than its bulk solution value. In addition to the classical double-layer effects discussed here, recent work of White and co-workers[47,48] suggests that at least two additional factors may have contributed to an error in the estimation of the heterogeneous electron transfer rate constant. Specifically, Norton et al. considered migration effects observed in cases where a charged species is reduced or oxidized at a spherical microelectrode with a radius comparable to the thickness of the diffuse double layer.[47] These calculations suggest that in our case an enhancement of current and a positive shift of the voltammograms may be expected as a result of an attractive electrostatic force between $Ru(NH_3)_6^{3+}$ and the electrode surface. This effect would lead then to an overestimation of the rate constant similar to the classical Frumkin effects. Current enhancement can indeed be observed in our experiments (involving surface concentrations of Q_{50} below 10^{-15} mol/cm^2) when KCl electrolyte concentration is decreased below 0.1 M. However, our experiments were carried out in 0.5 M KCl solutions and no decrease of current was observed when the electrolyte concentration was increased to 1.0 M. Recently, Smith and White considered similar migration effects resulting from a postulated breakdown of the electroneutrality conditions in the vicinity of microelectrodes of submicron dimensions.[48] Interestingly enough, the resulting shift in the position of the current voltage waves that might be expected in our experiments (and those reported by Penner et al.) would lead to an underestimation of the true rate constant of the electron transfer. These effects and a more careful examination of the electron transfer kinetics are the subjects of our current investigations.

Conclusions

Results presented here document the possibility of carrying out electrochemical reactions at a controlled number of single molecule gate sites purposefully incorporated in an otherwise impermeable L-B film on the electrode surface. Q_{50} molecules appear to create channels in the passivating $C_{18}SH/C_{18}OH$ layer which enable access of $Ru(NH_3)_6^{3+}$, a probe species, to the electrode surface. We considered and eliminated the possibilities of electron tunneling through the isoprenoid chain as well as the involvement of redox mediation of $Ru(NH_3)_6^{3+}$ reduction by the hydroquinone group of Q_{50}. On the basis of the

(36) Kuta, J.; Yeager, E. *Electroanal. Chem.* **1975**, *59*, 110.
(37) Peter, L. M.; Dürr, W.; Bindra, P.; Gerischer, H. *J. Electroanal. Chem.* **1976**, *71*, 31.
(38) Kulesza, P.; Jedral, T.; Galus, Z. *J. Electroanal. Chem.* **1980**, *109*, 141.
(39) Kawiak, J.; Jedral, T.; Galus, Z. *J. Electroanal. Chem.* **1983**, *145*, 163.
(40) Wipf, D. O.; Kristensen, E. W.; Deakin, M. R.; Wightman, R. M. *Anal. Chem.* **1988**, *60*, 306.
(41) Sabatani, E.; Rubinstein, I. *J. Phys. Chem.* **1987**, *91*, 6663.
(42) Penner, R. M.; Heben, M. J.; Longin, T. L.; Lewis, N. S. *Science* **1990**, *250*, 1118.
(43) Bard, A. J.; Faulkner, L. R. *Electrochemical Methods*; J. Wiley and Sons: New York, 1980; pp 540–544.
(44) Hamelin, A. in *Modern Aspects of Electrochemistry*; Conway, B. E.; White, R. E.; Bockris, J. O'M., Eds.; Plenum Press: New York, 1985; Vol. 16, Chapter 1, pp 1–101.
(45) Lecoeur, J.; Andro, J.; Parsons, R. *Surf. Sci.* **1982**, *114*, 320.
(46) Kolb, D. M.; Schneider, J. *Electrochim. Acta* **1986**, *31*, 929.
(47) Norton, J. D.; White, H. S.; Feldberg, S. W. *J. Phys. Chem.* **1990**, *94*, 6772.
(48) Smith, C. P.; White, H. S. *Anal. Chem.* **1993**, *65*, 3343.

A-S-T theory and the experimentally determined shift in the half-wave potential, the apparent heterogeneous rate constant of $Ru(NH_3)_6^{3+}$ at the Q_{50} gate molecules was determined to be 80 ± 2 cm/s. This high value is likely burdened with a positive error due to double layer effects. We explored the behavior of $C_{18}SH/C_{18}OH$ monolayers containing Q_{50} molecules for a broad range of concentrations. These mixed monolayers act as an array of molecular size microelectrodes when the Q_{50} concentration is below ca. 10^{-15} mol/cm^2. At higher concentrations negative deviations were observed in comparison to the calculated voltammetric response on the basis of A-S-T theory. The discrepancies were rationalized in terms of a loss of the gate molecules from the monolayer via a mechanism involving their aggregation and squeezing out.

This research opens new possibilities of inducing and controlling selectivity of the electrode/solution interface. Controlling access to the electrode surface on a single molecule basis is also a promising new approach in fundamental investigations of the molecular recognition phenomena.

Acknowledgment. We gratefully acknowledge the National Science Foundation for supporting this research under the grants CHE-9108378 and CHE-9422619.

LA941019G